

Cite this: *RSC Adv.*, 2013, **3**, 22461

# Helical self-assembly and nonlinear optical properties of optically active phthalocyanine derivatives bearing eight optically active diethyleneglycol mono-(S)-2-methylbutyl ether moieties on the $\beta$ -position of the phthalocyanine ring†

Jing Tian,<sup>a</sup> Lu Jing,<sup>a</sup> Lisha Ji,<sup>a</sup> Congcong Zhang,<sup>a</sup> Qingyun Liu<sup>b</sup> and Xiaomei Zhang<sup>\*a</sup>

Two phthalocyanine derivatives with eight peripheral chiral diethyleneglycol mono-(S)-2-methylbutyl ether moieties on the  $\beta$ -position of the phthalocyanine ring were prepared from the tetramerization of corresponding phthalonitriles, promoted by organic base 1,8-diazabicyclo[5.4.0]undec-7-ene (DBU). The self-assembly behavior of metal free phthalocyanine **1** and its copper congener **2** have been comparatively investigated by electronic absorption and circular dichroism (CD) spectroscopy, scanning electron microscopy (SEM), X-ray diffraction (XRD), and X-ray photoelectron spectroscopy (XPS). The metal free phthalocyanine **1** self-assembles into the right-handed screw-like aggregates (ca. 10  $\mu\text{m}$  length, 6  $\mu\text{m}$  width, and 1.5  $\mu\text{m}$  helical pitch), while, phthalocyaninato copper **2** self-assembled into left-handed fibrous aggregates (ca. 25  $\mu\text{m}$  length, 1  $\mu\text{m}$  width, and 0.7  $\mu\text{m}$  helical pitch). These results indicated the effect of metal-coordination bonds on the morphology and handedness of the self-assembled nanostructures. Further, excellent nonlinear optical (NLO) properties of both compounds were also revealed by a Z-scan experiment, which expand their applications in nonlinear optics.

Received 7th August 2013

Accepted 16th September 2013

DOI: 10.1039/c3ra44164d

[www.rsc.org/advances](http://www.rsc.org/advances)

## Introduction

Controlled helical self-assembly of functional conjugated molecules is a challenging topic for interdisciplinary research in the fields of chemistry, biology, and materials science because it provides spontaneous helical supramolecular structures with well-defined discrete morphology, whose property exhibition usually significantly depends on their morphology.<sup>1</sup> The major driving force operating in these precisely controlled helical supramolecular structures arises from the interplay of hydrogen bonding,  $\pi$ - $\pi$  stacking, metal coordination, electrostatic interactions, van der Waals, steric effects, hydrophobic interactions, chirality, and crystallization along with the involvement of growth kinetics.<sup>2</sup> On the basis of the interplay of these noncovalent interactions, a variety of elaborately designed molecules have been synthesized and fabricated into helical supramolecular structures.<sup>3</sup> However, precise control of helical

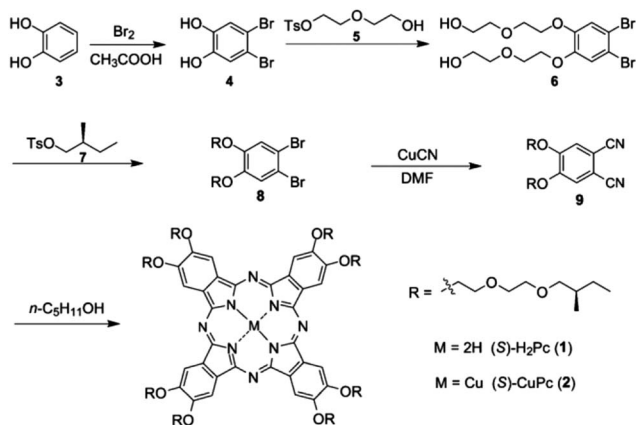
and exploring the functional properties of these optically active molecules at molecular and/or intermolecular level still remains a great challenge.

As one of the typical representatives of functional molecular materials with large conjugated electronic molecular structure, phthalocyanines often exhibit intriguing, peculiar, and tunable self-assembled, spectroscopic, photophysical, photochemical, particular nonlinear optical properties.<sup>4</sup> Its easily modified molecular structure renders it possible to incorporate various functional groups onto the peripheral positions and coordinate with almost all the metal ion, which not only provide enough room to tune the molecular functional properties by rationally molecular design, but also facilitate the introduction of various non-covalent interactions to tune the inter-molecular interaction of phthalocyanine molecules and in turn the morphology and functional properties of self-assembled supramolecular structures. To date, some phthalocyanine derivatives with excellent nonlinear optical properties have been designed and synthesized by breaking molecular symmetry, changing the size and degree of  $\pi$ -conjugated systems, and incorporating various donor-acceptor groups into phthalocyanine rings *etc.*<sup>5</sup> However, investigation of nonlinear optical properties of optically active phthalocyanine derivatives is rare, although chirality is believed to a desired selectivity to change the molecular symmetry.

<sup>a</sup>Department of Chemistry and Chemical Engineering, Shandong University, Jinan 250100, China. E-mail: zhangxiaomei@sdu.edu.cn

<sup>b</sup>School of Chemistry and Environmental Engineering, Shandong University of Science and Technology, Qingdao 266510, China

† Electronic supplementary information (ESI) available. See DOI: 10.1039/c3ra44164d



**Scheme 1** Synthesis of optically active phthalocyanine derivatives (S)-H<sub>2</sub>Pc (1) and (S)-CuPc (2).

With these ideas in mind, as our continuous strive towards design, synthesis, helical self-assembly, and exploring the functional properties of optically active phthalocyanine derivatives at molecular and/or intermolecular level,<sup>6</sup> in the present case, we describe the design and synthesis of two optically active phthalocyanine derivatives containing eight chiral diethyleneglycol mono-(S)-2-methylbutyl ether moieties at the β-position of phthalocyanine ring, namely metal free phthalocyanine derivative (S)-H<sub>2</sub>Pc (1) and its copper congener (S)-CuPc (2), Scheme 1. Their self-assembly behavior was comparatively investigated, revealing the effect of metal–ligand coordination bond interaction on the morphology and handedness of self-assembled nanostructures. Further, excellent nonlinear optical (NLO) properties of both compounds were also revealed by a Z-scan experiment.

## Results and discussion

### Synthesis and characterization of phthalocyanine derivatives 1 and 2

Optically active metal free phthalocyanine derivative, (S)-H<sub>2</sub>Pc (1), was prepared in good yield from compound (S)-9 in the presence of catalyst DBU in *n*-pentanol. Its corresponding phthalocyaninato copper complex (S)-CuPc (2) was obtained in good yield from the cyclic tetramerization of (S)-9 with Cu(OAc)<sub>2</sub> · 2H<sub>2</sub>O as template in the presence of DBU in refluxing *n*-pentanol. Satisfactory elemental analysis results were obtained for the newly prepared two compounds after repeated column chromatography followed by recrystallization. The MALDI-TOF mass spectrum of 1 and 2 showed intense signal corresponding to the molecular ion [M + 2H]<sup>2+</sup> and [M + H]<sup>+</sup>, respectively. The compounds 1 and 2 were also characterized with a range of spectroscopic methods.

### Electronic absorption, circular dichroism (CD) and fluorescence spectra

The electronic absorption and circular dichroism (CD) spectra of both phthalocyanine derivatives (S)-H<sub>2</sub>Pc (1) and (S)-CuPc (2) in CHCl<sub>3</sub> were recorded and the data are compiled in Table S1

(ESI<sup>†</sup>). As shown in Fig. 1B, compound 1 showed the typical metal free phthalocyanine electronic absorption spectra with the Soret band at 345 nm and the split Q bands at 639 nm and 674 nm with two shoulders at 580 nm and 618 nm, respectively. A weak absorption at around 413 nm is also observed, which is common for alkoxy-substituted phthalocyanines due to the *n* → π\* transition.<sup>7</sup> Upon complexation with copper metal ion, the increase in the molecular symmetry from C<sub>2h</sub> for (S)-H<sub>2</sub>Pc (1) to C<sub>4h</sub> for (S)-CuPc (2) induces the change in the electronic absorption spectrum from typical feature for metal free phthalocyanine to that for typical phthalocyaninato metal species (Fig. 1E).<sup>8</sup> As can be found, the Soret band of compounds 2 in CHCl<sub>3</sub> appeared at 337 nm and a very strong Q absorption is observed at 652 nm with a weak vibronic shoulder at 619 nm. The weak absorption at 405 nm is also due to the *n* → π\* transition. Corresponding to their electronic absorption spectra, a relatively weak negative CD signal in the Q absorption region of phthalocyanine chromophore were observed in the CD spectra of 1 and 2, Fig. 1A and C, respectively, indicating the effective chiral information transfer from the optically active diethyleneglycol mono-(S)-2-methylbutyl ether to the phthalocyanine chromophore at the molecular level. According to the chiral exciton theory,<sup>9</sup> if an optically inactive chromophore shows negatively induced CD in the wavelength region of its electronic absorption, then the asymmetric field surrounding the molecule is determined to be right-handed. In the present case, the appearance of negative CD signal in the Q absorption

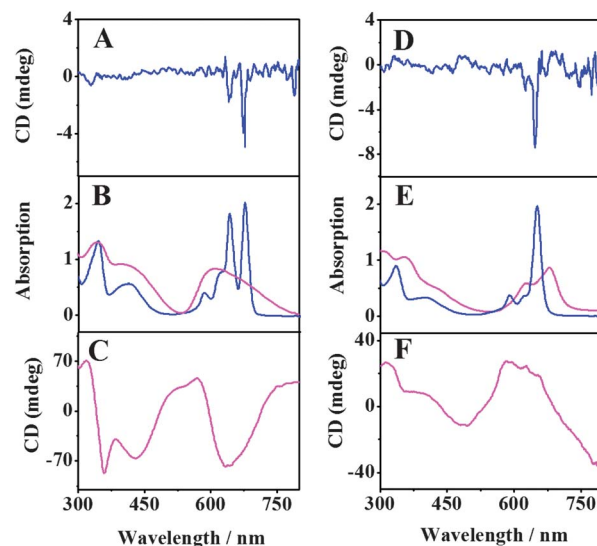


**Fig. 1** Circular dichroism (CD) spectra for (S)-H<sub>2</sub>Pc (1) ( $5 \times 10^{-5}$  mol L<sup>-1</sup>) in dilute chloroform solution (A); electronic absorption spectra of 1 in dilute chloroform solution ( $5 \times 10^{-5}$  mol L<sup>-1</sup>) (blue line) and aggregates fabricated from 1 dispersed in CHCl<sub>3</sub>/MeOH [1 : 3 (v/v)] ( $6 \times 10^{-5}$  mol L<sup>-1</sup>) (pink line) (B); CD spectra of aggregates fabricated from 1 ( $5 \times 10^{-5}$  mol L<sup>-1</sup>) dispersed in CHCl<sub>3</sub>/MeOH [1 : 3 (v/v)] ( $6 \times 10^{-5}$  mol L<sup>-1</sup>) (C); circular dichroism (CD) spectra for (S)-CuPc (2) ( $5 \times 10^{-5}$  mol L<sup>-1</sup>) in dilute chloroform solution ( $5 \times 10^{-5}$  mol L<sup>-1</sup>) (D); electronic absorption spectra of 2 in dilute chloroform solution ( $5 \times 10^{-5}$  mol L<sup>-1</sup>) (blue line) and aggregates fabricated from 2 dispersed in CHCl<sub>3</sub>/MeOH [1 : 3 (v/v)] ( $6 \times 10^{-5}$  mol L<sup>-1</sup>) (pink line) (E); CD spectra of aggregates fabricated from 2 dispersed in CHCl<sub>3</sub>/MeOH [1 : 3 (v/v)] ( $6 \times 10^{-5}$  mol L<sup>-1</sup>) (F).

region of **1** and **2** indicates that compounds **1** and **2** are all right-handed, implying the reverse chiral information transfer from the peripheral chiral diethyleneglycol mono-(*S*)-2-methylbutyl ether side chains to the phthalocyanine chromophore at the molecular level.

The electronic absorption and CD spectra of the aggregates formed from compounds **1** and **2** in CHCl<sub>3</sub>/MeOH [1 : 3 (v/v)] are also recorded and shown in Fig. 1. As shown in Fig. 1B, when metal free phthalocyanine **1** self-assembles into aggregates, both the Soret and Q bands for **1** lose some intensity. In particular, the Soret band for the aggregates takes a slight blue shift from 345 nm in chloroform to 341 nm in CHCl<sub>3</sub>/MeOH [1 : 3 (v/v)]. Meanwhile, the well-defined Q bands of metal free phthalocyanine **1** at 639 and 674 nm disappear and a very weak absorption band appears in the lower energy side of (639 + 674)/2 = 657 nm with the maximum at 598 nm in the aggregate electronic absorption spectrum. In comparison with the electronic absorption spectrum of **2** in dilute chloroform solution, both the Soret and Q absorption bands was found to be broadened in its aggregate electronic absorption spectrum and red-shift from 652 nm in CHCl<sub>3</sub> to 682 nm in CHCl<sub>3</sub>/MeOH [1 : 3 (v/v)], Fig. 1E. On the basis of Kasha's exciton theory,<sup>10</sup> blue-shift in the main absorption bands of (*S*)-H<sub>2</sub>Pc (**1**) upon aggregation reveals that the phthalocyanine molecules self-assemble into the H aggregates with a face-to-face molecular arrangement in their nano-structures. In contrast, the red-shifted absorption bands in the electronic absorption spectra of aggregates of **2** formed in CHCl<sub>3</sub>/MeOH [1 : 3 (v/v)], is typically a sign of the effective  $\pi$ - $\pi$  interaction between the (*S*)-CuPc molecules, indicating the formation of J aggregates and revealing a head-to-tail molecular arrangement in these nano-structures. In the CD spectra of compounds **1** and **2** aggregates formed in CHCl<sub>3</sub>/MeOH [1 : 3 (v/v)], Fig. 1C and F, perfect mirroring Cotton effect was observed, indicating the successfully chiral expression on the phthalocyanine chromophore at the supramolecular level. According to the semiempirical method developed by Nakaniishi and co-workers,<sup>11</sup> the given sign of coupling and the direction of dipole moments can be used to determine the chirality of stacked phthalocyanine molecules in aggregates. In general, the circular dichroism spectrum featuring a bisignate Cotton effect showing positive feature at longer wavelength and negative one at shorter wavelength indicates the right-handed chirality of the dipole moments (positive chirality), while conversely left-handed chirality (negative chirality). In the present case, a negative bisignate Cotton effect 572(+)/634(-) with the crossovers at 603 nm for **1** and 586(-)/774(+) with the crossovers at 680 nm for **2** were observed, corresponding to the Q-band of compounds **1** and **2** aggregates, respectively, indicating a left-handed (*M*) helical arrangement of corresponding molecules in a stack of phthalocyanine chromophores in the aggregates. The formation of the supermolecular helicity, observed from the circular dichroism spectroscopy, is unequivocally confirmed by SEM analysis of the **1** or **2** aggregates as detailed below.

The fluorescence spectra of compounds **1** and **2** in chloroform and methanol are compared in Fig. S1 (ESI<sup>†</sup>). Fluorescence quantum yields ( $\Phi_f$ ) were determined by using zinc

phthalocyanine ( $\Phi_f = 0.30$ ) in benzene as standard following the literature method.<sup>12</sup> Fluorescence quantum yields for compounds **1** and **2** in CHCl<sub>3</sub>/MeOH [1 : 3 (v/v)] are calculated as 0.19 and 0.31, respectively. The significant fluorescence quenching, observed for **1** and **2** in CHCl<sub>3</sub>/MeOH [1 : 3 (v/v)], indicates the formation of aggregates with strong intermolecular  $\pi$ - $\pi$  interactions between the phthalocyanine rings of these two compounds, respectively. In comparison with compound **1**, the uncompleted fluorescence quenching for **2** in CHCl<sub>3</sub>/MeOH [1 : 3 (v/v)] obviously suggests the formation of aggregates with relative weak  $\pi$ - $\pi$  interaction between the phthalocyanine rings of **2**, implying the increased distance (perpendicular to the phthalocyanine **2** molecules) due to the formation of additional metal-ligand (Cu-O<sub>alkoxy</sub>) coordination bonds between the alkoxy substituents of one phthalocyaninato copper molecule and central copper ion of the neighbouring phthalocyanine molecule.

### Morphology of the aggregates

The evidence for the formation of the helical aggregates was also provided by scanning electron microscopy (SEM). Samples were prepared by casting a drop of sample solution onto SiO<sub>2</sub> substrate. As can be found in Fig. 2, both of compounds **1** and **2** self-assembled into helical aggregates, with average 10  $\mu$ m length and 6  $\mu$ m width for **1** and 25  $\mu$ m length and 1  $\mu$ m width for **2**. In detail, as shown in the high-magnification SEM image, Fig. 2a and b, the screw-like aggregates formed from **1** are right-handed with the average helical pitch of about 1.5  $\mu$ m. However, the fibrous aggregates formed from **2** are left-handed with the average helical pitch of about 0.7  $\mu$ m. As detailed in the electronic absorption and circular dichroism (CD) spectroscopy section, the CD signal of aggregates fabricated from **1** and **2** demonstrated that the molecules of **1** and **2** within an elementary fiber are organized into a left-handed helix. Clearly, the present SEM image of aggregates fabricated from **1** is converse with the observed CD signal and the width of both aggregates fabricated from **1** and **2** are wider than the length of molecules. These results clearly reveal the hierarchical self-assembling nature of the two compounds. At the first stage, the phthalocyanine

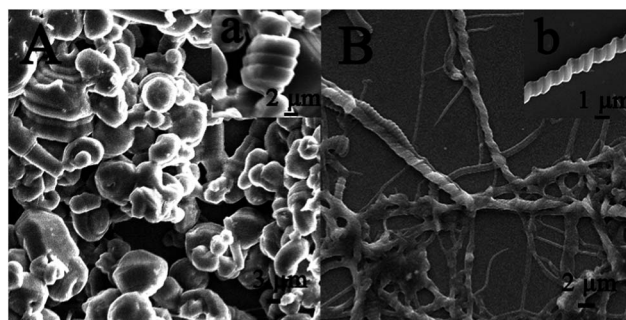


**Fig. 2** Nano-particles fabricated from (*S*)-H<sub>2</sub>Pc (**1**) in CHCl<sub>3</sub>/MeOH [1 : 3 (v/v)] observed by SEM (A); high-magnification SEM image fabricated from **1**, showing right-handed screw-like nano-structure (a). Nano-fibers fabricated from (*S*)-CuPc (**2**) in CHCl<sub>3</sub>/MeOH [1 : 3 (v/v)] observed by and SEM (B). High-magnification SEM image fabricated from **2**, showing left-handed fibrous nano-structure (b).

compounds self-assemble into one-dimensional helices with left-handed helical arrangement, which as elementary building blocks further stack into highly ordered fibrous nanostructures with the same and/or the converse helicity, respectively.

### X-ray diffraction patterns of the aggregates

The internal structure of self-assembled nanostructures were further investigated by X-ray diffraction (XRD) technique. Fig. 3 exhibits the diffraction patterns of the self-assembled nanostructures formed from **1** and **2**, respectively. As can be seen from Fig. 3A, the XRD diagram of the aggregates formed from **1** shows strong and rich diffraction peaks at  $2\theta = 3.42^\circ$  (corresponding to 2.58 nm),  $3.62^\circ$  (2.44 nm),  $4.12^\circ$  (2.14 nm),  $5.06^\circ$  (1.74 nm), and  $8.40^\circ$  (1.05 nm) in the low angle range and a diffraction peak at  $2\theta = 12^\circ$  (corresponding to 0.76 nm) in the wide angle range. On the basis of the  $hkl$  indexation of the observed refraction lines, these diffraction peaks are ascribed to those from the (200), (010), (110), (300), (500), and (700) planes of a 2D rectangular column packing with lattice parameter of  $a = 5.16$  nm and  $b = 2.44$  nm. In the wide angle region, the XRD pattern also presents two diffraction peaks at  $2\theta = 20.8^\circ$  (corresponding to 0.43 nm) and  $29.16^\circ$  (0.31 nm). The former diffraction was due to the fluid like packing of chiral side chains of **1**, while the latter one assigned to the stacking distance between neighboring phthalocyanine **1** molecules in the direction parallel to the tetrapyrrole rings.<sup>13</sup>

The XRD diagram of the aggregates formed from **2**, Fig. 3B, gives three diffraction peaks at  $2\theta = 3.30^\circ$  (corresponding to 2.68 nm),  $5.70^\circ$  (1.55 nm), and  $6.60^\circ$  (1.34 nm) in the low angle range in a ratio of 1 : 0.58 : 0.5, indexing as the diffractions from the (100), (110), and (200) planes of a 2D hexagonal

column packing with lattice parameter of  $a = 2.68$  nm.<sup>14</sup> In the wide angle range, one higher order diffraction for (110) plane at  $0.78$  (120) was also observed. Similar to the aggregates formed from **1**, two additional diffraction peaks at  $0.43$  and  $0.31$  nm, corresponding to the fluid like packing of chiral side chains of **2** and the stacking distance between neighboring molecules in the direction parallel to the tetrapyrrole rings were also observed. In addition, in the wide angle region, the XRD pattern also presents one sharp refraction at  $0.30$  nm. As indicated below, the IR and XPS spectroscopic results indicate the formation of Cu–O<sub>alkoxy</sub> coordination bond between the alkoxy substituents of one phthalocyaninato copper molecule and central copper ion of neighbouring phthalocyanine molecule. Therefore, the diffraction peak at  $0.30$  nm are assigned to the Cu–O<sub>alkoxy</sub> coordination bond length between Cu<sup>2+</sup> atom of phthalocyaninato copper molecule and the oxygen atoms of neighbouring phthalocyanine molecule below or above the phthalocyanine ring.

### XPS analysis

To confirm the existence of Cu–O<sub>alkoxy</sub> coordination bonds between oxygen atom of the phthalocyaninato copper molecule and copper center of neighboring molecule in the aggregates of **2**, X-ray photoelectron spectroscopy (XPS) was employed to detect the copper ion circumstance. Fig. S2 (ESI<sup>†</sup>) display the XPS spectra of **2** in chloroform and aggregates formed from **2** in CHCl<sub>3</sub>/MeOH [1 : 3 (v/v)], respectively. As expected, the two samples show typical signals for the Cu<sup>2+</sup> ion in their XPS spectra. In detail, the strong absorption peak at 937 and the weak absorption peaks at 957 for monomeric complex **2** attributed to the Cu<sub>2p3/2</sub> and its satellite peak, respectively.<sup>15</sup> However, the Cu<sup>2+</sup> signals in the XPS spectra of **2** aggregates formed in CHCl<sub>3</sub>/MeOH [1 : 3 (v/v)] take obvious shift to the lower bonding energy direction in comparison with those of **2** in chloroform, indicating the change of Cu<sup>2+</sup> circumstance after self-assembly process due to the formation of Cu–O<sub>alkoxy</sub> coordination bonds in the aggregates of **2** formed.

### IR spectra

The IR spectra of these two phthalocyanine derivatives and their self-assembled aggregates obtained are shown in Fig. S3 and S4 (ESI<sup>†</sup>). The similar feature in the IR spectra of the aggregates to that of corresponding compounds for (*S*)-H<sub>2</sub>Pc (**1**) and (*S*)-CuPc (**2**) unambiguously confirms the composition of aggregates from corresponding phthalocyanine compounds. In detail, in the IR spectrum of metal free phthalocyanine **1** and phthalocyaninato copper complex **2**, two relatively sharp absorptions at *ca.* 1214 and 1026 cm<sup>-1</sup> for **1** and 1217 and 1066 cm<sup>-1</sup> for **2** are assigned to the symmetric and asymmetric C–O–C bonding stretching vibration, respectively, Fig. S3A and S4A (ESI<sup>†</sup>). Similar absorption peaks at 1214 and 1027 cm<sup>-1</sup> are also observed in the IR spectrum of aggregates fabricated from **1**, Fig. S3B (ESI<sup>†</sup>). However, due to the formation of Cu–O<sub>alkoxy</sub> coordination bond of oxygen atom in the diethyleneglycol mono-(*S*)-2-methylbutyl ether side chains in **2** molecule with copper center of neighboring **2** molecule, the typical C–O–C

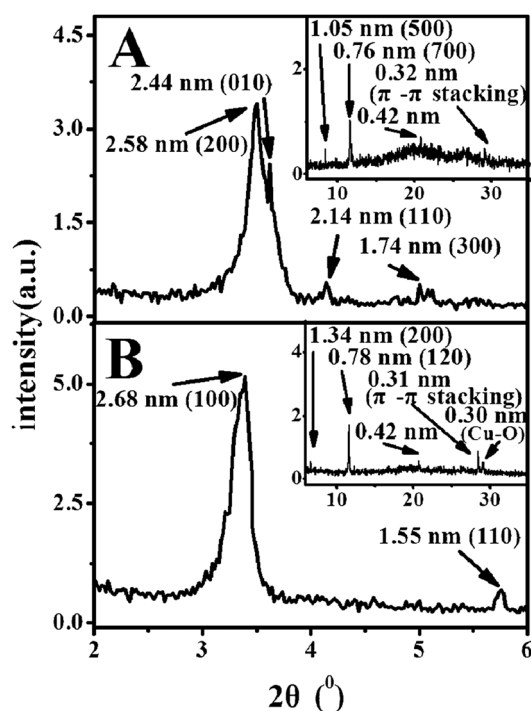


Fig. 3 XRD profile of aggregates fabricated from (*S*)-H<sub>2</sub>Pc (**1**) (A) and (*S*)-CuPc (**2**) (B).

stretching vibration are shifted to lower frequency at 1218 and 1068  $\text{cm}^{-1}$ , respectively, Fig. 4B, implying the formation of  $\text{Cu-O}_{\text{alkoxy}}$  coordination bond between the central copper ion of the phthalocyaninato copper to the oxygen atom of the adjacent phthalocyaninato copper molecule.

### Nonlinear optical properties

The third-order nonlinear absorption of compounds **1** and **2** were measured by the Z-scan technique. The open-aperture Z-scan experimental setup is shown as previously described in detail.<sup>16</sup> Before the measurement, the system was calibrated by  $\text{CS}_2$  in a quartz cell as reference. In the measurements, a mode-locked Nd:YAG laser system (PY61C-10, Continuum) was used at the wavelength of 532 nm with the pulse width of 20 ps and the repetition rate of 10 Hz. The energy of laser of the sample is 19 uJ, the laser beam was focused with an  $f = 15$  cm lens and the beam waist radius ( $w_0$ ) was measured to be 40.0  $\mu\text{m}$  and the corresponding Rayleigh length is 3.9 mm. The thickness of a quartz cell containing the sample is 1 mm which is less than the Rayleigh length of the laser beam. The ultraviolet absorption spectrum of the samples was shown as Fig. S5 (ESI<sup>†</sup>). It is noteworthy that the measurements on the reference solution in the cell were also performed under the same measurement conditions to verify that the valleys and the peaks in the Z-scan curves originated from the material instead from the solvent or the quartz cell.<sup>17</sup>

The nonlinear optical properties of compound **1** and **2** in chloroform solution were obtained by a Z-scan experiment under an open-aperture, Fig. 4. The concentrations of the samples were  $1 \times 10^{-4}$  mol  $\text{L}^{-1}$  and the NLO absorption data was calculated according to the reported equations.<sup>18</sup> As can be

seen, both of compound **1** and **2** in chloroform solution exhibits excellent reverse saturated absorption optical property under an open-aperture configuration and the corresponding nonlinear absorption coefficient were  $1.18 \times 10^{-9}$  m  $\text{W}^{-1}$  and  $1.42 \times 10^{-9}$  m  $\text{W}^{-1}$ , which was among the best results ever reported for porphyrin and phthalocyanine derivatives<sup>19,20</sup> and then exhibit their potential applications as nonlinear optics devices.

### Conclusion

In the present paper, optically active metal free phthalocyanine and its copper complex were designed and synthesized. The self-assembly behavior of the two phthalocyanine derivatives have been comparatively studied. In comparison with compound **1**, which hierarchically self-assemble into right-handed screw-like aggregates with average 10  $\mu\text{m}$  length, 6  $\mu\text{m}$  width, and 1.5  $\mu\text{m}$  helical pitch, compound **2** self-assembled into more longer left-handed fibrous aggregates with 25  $\mu\text{m}$  in length, 1  $\mu\text{m}$  in width and 0.7  $\mu\text{m}$  helical pitch due to the additionally formed metal-coordination bonds between  $\text{Cu}^{2+}$  atom of phthalocyaninato copper molecule and the oxygen atoms of neighbouring phthalocyanine molecule. Further, excellent nonlinear optical (NLO) properties of both compounds were also revealed by a Z-scan experiment. The present result represents few of the helical self-assembly fabricated from phthalocyanine derivatives containing chiral substituents on the phthalocyanine ring and will be helpful towards rational design and preparation of nanoscale chiral function materials and nonlinear optical materials.

### Experimental section

#### General

1,8-Diazabicyclo[5.4.0]undec-7-ene (DBU) was purchased from Aldrich. 1-Pentanol and DMF were freshly distilled just before use. Column chromatography was carried out on silica gel (Merck, Kieselgel 60, 200–300 mesh) with the indicated eluents. Optically pure (*S*)-2-methyl-1-butanol (>99% ee) were obtained from Shanghai DEMO medical technology limited Company. All other reagents and solvents were of reagent grade form and used as received. Compounds **3**–**7** were prepared according to the published procedures.<sup>21,22</sup>

#### Self-assembled aggregates fabrication

The self-assembled aggregates of the phthalocyanine derivatives **1** and **2** were fabricated by the phase transfer method according to the following procedure.<sup>23</sup> A minimum volume (50  $\mu\text{L}$ ) of concentrated chloroform solution of compounds **1** and **2** (1 mM), respectively, were injected rapidly with a micro injector into a large volume of  $\text{CHCl}_3/\text{MeOH}$  [1 : 3 (v/v)] (1 mL) and subsequently mixed. After the solution was allowed to equilibrate at ambient temperature for two days, the loose aggregates were observed. These precipitates were then transferred to the carbon-coated grid by pipetting for SEM observations. These procedures and results were stable and

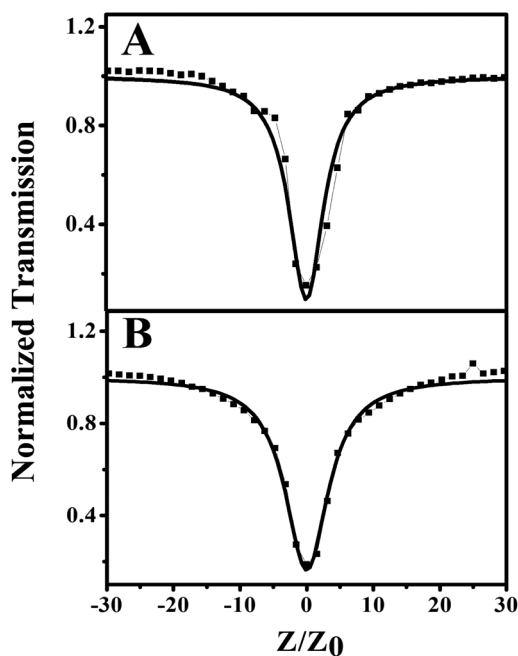


Fig. 4 Nonlinear optical (NLO) absorptive properties of (*S*)- $\text{H}_2\text{Pc}$  (**1**) (A) and (*S*)- $\text{CuPc}$  (**2**) (B) in the solution pattern under an open-aperture configuration.

reproducible under the experimental conditions described above.

### Measurements

$^1\text{H}$  NMR spectrum was recorded on a Bruker DPX 300 spectrometer (300 MHz) in  $\text{CDCl}_3$  using the residual solvent resonance of  $\text{CHCl}_3$  at 7.26 ppm relative to  $\text{SiMe}_4$  as internal reference. Fourier transform infrared spectra (IR) were recorded in KBr pellets with  $2\text{ cm}^{-1}$  resolution using a  $\alpha$ ALPHA-T spectrometer. MALDI-TOF mass spectrum was taken on a Bruker BIFLEX III ultra-high resolution Fourier transform ion cyclotron resonance (FT-ICR) mass spectrometer with  $\alpha$ -cyano-4-hydroxycinnamic acid as matrix. Elemental analysis was performed on an Elementar Vavio El III. Circular dichroism (CD) measurements were carried out on a JASCO J-810 spectropolarimeter. Low-angle X-ray diffraction (XRD) measurements were carried out on a Rigaku D/max-cB X-ray diffractometer. The fluorescence spectra were recorded on a RF-5301Pc fluorometer with excitation and emission slits of 10 nm. Scanning electron microscopic (SEM) images were obtained on a JEOL JSM-6700F. For SEM imaging, C (1–2 nm) was sputtered onto these grids to prevent charging effect and improve the image clarity.

### Preparation of dibromobenzene derivative (S)-8

Compounds **6** (1.76 g, 4 mmol), **7** (2.13 g, 8.8 mmol), BuOK (0.986 g, 8.8 mmol) and 20 mL of freshly distilled THF were placed in a 50 mL round-bottom flask. After refluxed for 12 h, the reaction mixture was poured into water and extracted with dichloromethane, then dried with anhydrous sodium sulfate. After evaporated dichloromethane, the residue was purified by silica gel chromatography with ethyl acetate/petroleum ether (60–90 °C) (1 : 5) as the eluent and give the compound (S)-**8** as a viscous oil (1.98 g, 85%).  $^1\text{H}$  NMR (300 MHz) ( $\text{CDCl}_3$ ): 0.86–0.90 (m, 12H), 1.04–1.18 (m, 2H), 1.37–1.48 (m, 2H), 1.57–1.70 (m, 2H), 3.19–3.24 (m, 2H), 3.29–3.24 (m, 2H), 3.56–3.59 (t,  $J = 4.95$  Hz, 4H), 3.68–3.71 (t,  $J = 4.8$  Hz, 4H), 3.83–3.86 (t,  $J = 4.8$  Hz, 4H), 4.11–4.14 (t,  $J = 4.95$  Hz, 4H), 7.14 (s, 2H).

### Preparation of 1,2-phthalodinitrile derivative (S)-9

A mixture of (S)-**8** (1 g, 1.71 mmol), CuCN (0.46 g, 5.13 mmol), and DMF (10 mL) in a 50 mL round-bottom flask were refluxed under nitrogen for 8 h. The reaction mixture was cooled to room temperature and then poured into 80 mL aqueous ammonia. After blowing air for 2 h, the mixture was extracted with toluene (50 mL  $\times$  3). The combined organic layers were washed with water, dried over anhydrous sodium sulfate and then concentrated. The residue was purified by silica gel chromatography with ethyl acetate/petroleum ether (60–90 °C) (1 : 15) as the eluent and give the product (S)-**9** as a viscous oil (0.65 g, 79%).  $^1\text{H}$  NMR (300 MHz) ( $\text{CDCl}_3$ ): 0.90–0.96 (m, 12H), 1.15–1.20 (m, 2H), 1.53–1.58 (m, 2H), 1.95–1.99 (m, 2H), 3.41–3.46 (m, 2H), 3.52–3.56 (m, 2H), 3.77–3.80 (t,  $J = 4.95$  Hz, 4H), 3.88–3.93 (t,  $J = 4.8$  Hz, 4H), 4.15–4.20 (t,  $J = 4.8$  Hz, 4H), 4.30–4.35 (t,  $J = 4.95$  Hz, 4H), 7.68 (s, 2H).

### Preparation of optically active metal free phthalocyanine derivative (S)-H<sub>2</sub>Pc (1)

Wiped lithium (2.94 mg, 0.42 mmol) which was cut into thin strips and *n*-pentanol (5 mL) were placed in a 150 mL round-bottom flask, heated to 60–70 °C under nitrogen to melt lithium. Then the reaction system was cooled to room temperature, (S)-**9** (100 mg, 0.21 mmol) was added in the reaction system and re-heated to 150 °C under nitrogen to reaction for 6 h. After cooling to room temperature, the reaction mixture was removed to a 150 mL round-bottom flask, methanol (100 mL) was added and then acetic acid (2 mL) was added dropwise with stirring. The crystalline residue was collected by filtration, washed with methanol, and purified by silica gel column chromatography with  $\text{CHCl}_3/\text{MeOH}$  [100 : 1 (v/v)] as eluent. The crude product was purified by recrystallization from  $\text{CHCl}_3/\text{MeOH}$ , giving pure compound **1** as green powder (38.6 mg, 38%).  $^1\text{H}$  NMR (300 MHz) ( $\text{CDCl}_3$ ): 0.86–0.98 (m, 48H), 1.11–1.18 (m, 8H), 1.45–1.51 (m, 8H), 1.58 (s, 4H), 1.69–1.74 (m, 8H), 3.29–3.33 (m, 8H), 3.39–3.42 (m, 8H), 3.73–3.76 (t,  $J = 3.75$  Hz, 16H), 3.96–3.98 (t,  $J = 3.6$  Hz, 16H), 4.25–4.27 (t,  $J = 3.6$  Hz, 16H), 4.78–4.79 (t,  $J = 3.6$  Hz, 16H), 8.75–8.80 (br, 8H). MS: calcd for  $\text{C}_{104}\text{H}_{162}\text{N}_8\text{O}_{24}$  ( $\text{M}^+$ ) 1908.17; found  $m/z$  1908.53. Anal. calcd (%) for  $\text{C}_{104}\text{H}_{162}\text{N}_8\text{O}_{24}$ : C, 65.40; H, 8.49; N, 5.87; found: C, 65.48; H, 8.44; N, 5.83.

### Preparation of optically active phthalocyaninato copper derivative (S)-CuPc (2)

A mixture of (S)-**9** (476 g, 1 mmol),  $\text{Cu}(\text{OAc})_2 \cdot 2\text{H}_2\text{O}$  (100 g, 0.5 mmol), and DBU (0.004 g, 0.023 mmol) in *n*-pentanol (5 mL) was heated to reflux under nitrogen for 6 h. Then the reaction mixture was cooled to room temperature. After *n*-pentanol being distilled off under reduced pressure, the residue was dissolved in chloroform and then purified by silica gel column chromatography with  $\text{CHCl}_3/\text{MeOH}$  [200 : 1 (v/v)] as eluent, the crude product was purified by recrystallization from  $\text{CHCl}_3/\text{MeOH}$ , giving complex **2** as dark green powder (184.59 mg, 37.5%). The  $^1\text{H}$  NMR spectra of compound **2** is not distinct as (S)-H<sub>2</sub>Pc (**1**) due to the paramagnetic of  $\text{Cu}^{2+}$ .

### Acknowledgements

Financial support from the Natural Science Foundation of China (Grant no. 211711061).

### References

- (a) G. de la Torre, G. Bottari, U. Hahn and T. Torres, in *Structure and Bonding: Functional Phthalocyanine Molecular Materials*, ed. J. Jiang, Springer, Heidelberg, 2010, vol. 135, pp. 1–45; (b) M. A. Mateos-Timoneda, M. Crego-Calama and D. N. Reinhoudt, *Chem. Rev.*, 2004, **33**, 363–372; (c) J. Cornelissen, A. E. Rowan, R. J. M. Nolte and N. Sommerdijk, *Chem. Rev.*, 2001, **101**, 4039–4070; (d) B. W. Messmore, P. A. Sukerkar and S. I. Stupp, *J. Am. Chem. Soc.*, 2005, **127**, 7992–7993; (e) T. Kato, T. Matsuoka, M. Nishii, Y. Kamikawa, K. Kanie, T. Nishimura,

- E. Yashima and S. Ujiie, *Angew. Chem., Int. Ed.*, 2004, **43**, 1969–1972; (f) Z. Guo, I. De. Cat, B. V. Averbeke, J. Lin, G. Wang, H. Xu, R. Lazzaroni, D. Beljonne, E. W. Meijer, A. P. H. J. Schenning and S. De. Feyter, *J. Am. Chem. Soc.*, 2011, **133**, 17764–17771.
- 2 (a) Ajayaghosh and V. K. Praveen, *Acc. Chem. Res.*, 2007, **40**, 644–656; (b) J. A. A. W. Elemans, R. van Hameren, R. J. M. Nolte and A. E. Rowan, *Adv. Mater.*, 2006, **18**, 1251–1266; (c) G. Lu, Y. Chen, Y. Zhang, M. Bao, Y. Bian, X. Li and J. Jiang, *J. Am. Chem. Soc.*, 2008, **130**, 11623–11630; (d) S. Cui, H. Liu, L. Gan, Y. Li and D. Zhu, *Adv. Mater.*, 2008, **20**, 2918–2925; (e) Huang, Y. Li, Y. Song, Y. Li, H. Liu and D. Zhu, *Adv. Mater.*, 2010, **22**, 3532–3536.
- 3 (a) R. Oda, M. Schmutz, S. J. Candau and F. C. MacKintosh, *Nature*, 1999, **399**, 566–569; (b) E. D. Sone, E. R. Zubarev and S. I. Stupp, *Angew. Chem., Int. Ed.*, 2002, **41**, 1706–1709; (c) H. Fenniri, B.-L. Deng and A. E. Ribbe, *J. Am. Chem. Soc.*, 2002, **124**, 11064–11072; (d) T. Giorgi, S. Lena, P. Mariani, M. A. Cremonini, S. Masiero, S. Pieraccini, J. P. Rabe, P. Samori, G. P. Spada and G. Gottarelli, *J. Am. Chem. Soc.*, 2003, **125**, 14741–14749; (e) J. Xiao, J. Xu, S. Cui, H. Liu, S. Wang and Y. Li, *Org. Lett.*, 2008, **10**, 645–648; (f) T. Kato, T. Matsuoka, M. Nishii, Y. Kamikawa, K. Kanie, T. Nishimura, E. Yashima and S. Ujiie, *Angew. Chem., Int. Ed.*, 2004, **43**, 1969–1972.
- 4 (a) G. D. Pantos, J. L. Wietor and J. K. M. Sanders, *Angew. Chem., Int. Ed.*, 2007, **46**, 2238–2240; (b) J. J. L. M. Cornelissen, A. E. Rowan, R. J. M. Nolte and N. A. J. M. Sommerdijk, *Chem. Rev.*, 2001, **101**, 4039–4070; (c) A. R. A. Palmans, J. A. J. M. Vekemans, E. E. Havinga and E. W. Meijer, *Angew. Chem., Int. Ed.*, 1997, **36**, 2648–2651; (d) S. I. Stupp, V. LeBonheur, K. Walker, L. S. Li, K. E. Huggins, M. Keser and A. Amstutz, *Science*, 1997, **276**, 384–389; (e) L. J. Prins, J. Huskens, D. F. Jong and P. Timmerman, *Nature*, 1999, **398**, 498–502; (f) L. Ma, Y. Zhang and P. Yuan, *Opt. Express*, 2010, **18**(17), 17666–17671.
- 5 (a) G. de la Torre, P. Vázquez, F. Agulló-López and T. Torres, *Chem. Rev.*, 2004, **104**, 3723; (b) M. O. Senge, M. Fazekas, E. G. A. Notaras, W. J. Blau, M. Zawadzka, O. B. Locos and E. M. Ni Mhuircheartaigh, *Adv. Mater.*, 2007, **19**, 2737; (c) Y. Xu, Z. Liu, X. Zhang, Y. Wang, J. Tian, Y. Huang, Y. Ma, X. Zhang and Y. Chen, *Adv. Mater.*, 2009, **21**, 1275; (d) Z. Liu, J. Tian, Z. Guo, D. Ren, F. Du, J. Zheng and Y. Chen, *Adv. Mater.*, 2008, **20**, 511; (e) C. Bucher, C. H. Devillers, J. C. Moutet, G. Royal and E. Saint-Aman, *Coord. Chem. Rev.*, 2009, **253**, 21.
- 6 (a) J. J. L. M. Cornelissen, M. Fisher, N. A. J. M. Sommerdijk and R. J. M. Nolte, *Science*, 1998, **280**, 1427–1430; (b) A. de la Escosura, M. V. Martinez-Diaz, P. Thordarson, A. E. Rowan, R. J. M. Nolte and T. Torres, *J. Am. Chem. Soc.*, 2003, **125**, 12300–12308; (c) M. Kimura, H. Narikawa, K. Ohta, K. Hanabusa, H. Shirai and N. Kobayashi, *Chem. Mater.*, 2002, **14**, 2711–2717; (d) Y. Zhang, H. Dong, Q. Tang, S. Ferdous, F. Liu, S. C. B. Mannsfeld, W. Hu and A. L. Briseno, *J. Am. Chem. Soc.*, 2011, **132**, 11580–11584; (e) L. Wu, Q. Wang, J. Lu, Y. Bian, J. Jiang and X. Zhang, *Langmuir*, 2010, **26**, 7489–7497; (f) R. Gleiter, D. Werz and B. Rausch, *Chem.–Eur. J.*, 2003, **9**, 2676–2683.
- 7 (a) Y. Zhang, X. Zhang, Z. Liu, Y. Bian and J. Jiang, *J. Phys. Chem. A*, 2005, **109**, 6363–6370; (b) N. Sheng, R. Li, C. F. Choi, W. Su, D. K. P. Ng, X. Cui, K. Yoshida, N. Kobayashi and J. Jiang, *Inorg. Chem.*, 2006, **45**, 3794–3802.
- 8 Y. Gao, Y. Chen, R. Li, Y. Bian, X. Li and J. Jiang, *Chem.–Eur. J.*, 2009, **15**, 13241–13252.
- 9 (a) H. Harada and K. Nakanishi, *Circular Dichroic Spectroscopy, Exciton Coupling in Organic Stereochemistry*, University Science Books, New York, 1983; (b) N. Kobayashi, *Chem. Commun.*, 1998, 487–488.
- 10 M. Kasha, H. R. Rawls and M. A. El-Bayoumi, *Pure Appl. Chem.*, 1965, **11**, 371–392.
- 11 (a) N. Berova, K. Nakanishi and R. Woody, *Circular Dichroism: Principles and Applications*, Wiley-VCH, New York, 2000, 2nd edn, pp. 337–382; (b) A. L. Hofacker and J. R. Parquette, *Angew. Chem., Int. Ed.*, 2005, **44**, 1053–1057; (c) M. Balaz, A. E. Holmes, M. Benedetti, P. C. Rodriguez, N. Berova, K. Nakanishi and G. Proni, *J. Am. Chem. Soc.*, 2005, **127**, 4172–4173; (d) V. V. Borovkov, J. M. Lintuluoto, M. Fujiki and Y. Inoue, *J. Am. Chem. Soc.*, 2000, **122**, 4403–4407.
- 12 D. J. Darwent, P. Douglas, A. Harriman, G. Porter and M. C. Richoux, *Coord. Chem. Rev.*, 1982, **44**, 83–126.
- 13 (a) L. Wu, Q. Wang, J. Lu, Y. Bian, J. Jiang and X. Zhang, *Langmuir*, 2010, **26**, 7489–7497; (b) W. Lv, X. Wu, Y. Bian, J. Jiang and X. Zhang, *ChemPhysChem*, 2009, **10**, 2725–2732; (c) R. Sun, L. Wang, J. Tian, X. Zhang and J. Jiang, *Nanoscale*, 2012, **4**, 6990–6996.
- 14 S. Laschat, A. Baro, N. Steinke, F. Giesselmann, C. Hagele, G. Scalia, R. Judele, E. Kapatsina, S. Sauer, A. Schreivogel and M. Tosoni, *Angew. Chem., Int. Ed.*, 2007, **46**, 4832–4887.
- 15 (a) M. Krzywiecki, L. Grzadziel, L. Ottaviano, P. Parisse, S. Santucci and J. Szuber, *Mater. Sci.-Pol.*, 2008, **26**(2), 288–294; (b) L. Lozzi, L. Ottaviano and S. Santucci, *Surf. Sci.*, 2001, **470**, 265–274; (c) S. Carniato, G. Dufour, Y. Luo and H. Ågren, *Phys. Rev. B: Condens. Matter Mater. Phys.*, 2002, **66**, 265–274.
- 16 Y. Chen, M. Hanack, Y. Araki and O. Ito, *Chem. Soc. Rev.*, 2005, **34**, 517–529.
- 17 (a) M. Sherk-Bahae, A. A. Said and E. W. Van Stryland, *Opt. Lett.*, 1989, **14**, 955; (b) H. Liu, J. Xu and Y. Li, *Acc. Chem. Res.*, 2010, **43**, 1496–1508; (c) J. Xu, S. Semin, D. Niedzialek, P. H. Kouwer, E. Fron, E. Coutino, M. Savoini, Y. Li, J. Hofkens, H. Uji-I, D. Beljonne, T. Rasing and A. E. Rowan, *Adv. Mater.*, 2013, **25**, 2084.
- 18 M. Sherk-Bahae, A. A. Said, T. H. Wei, D. J. Hagan and E. W. Van Stryland, *IEEE J. Quantum Electron.*, 1990, **26**, 760.
- 19 M. O. Senge, M. Fazekas, E. G. A. Notaras, *et al.*, *Adv. Mater.*, 2007, **19**(19), 2737–2774.
- 20 G. de la Torre, P. Vázquez, F. Agulló-López and T. Torres, *Chem. Rev.*, 2004, **104**, 3723–3750.
- 21 H. Liu, C. Chen, M. Ai, A. Gong, J. Jiang and F. Xi, *Tetrahedron: Asymmetry*, 2000, **11**, 4915–4922.
- 22 L. Wu, Q. Wang, J. Lu, Y. Bian, J. Jiang and X. Zhang, *Langmuir*, 2010, **26**, 7489–7497.

- 23 (a) K. Balakrishnan, A. Datar, R. Oitker, H. Chen, J. Zuo and L. Zang, *J. Am. Chem. Soc.*, 2005, **127**, 10496–10497; (b) W. Su, Y. Zhang, C. Zhao, X. Li and J. Jiang, *ChemPhysChem*, 2007, **8**, 1857–1862; (c) G. Lu, X. Zhang, X. Cai and J. Jiang, *J. Mater. Chem.*, 2009, 2417–2424; (d) X. Gong, T. Milic, C. Xu, J. D. Batteas and C. M. Drain, *J. Am. Chem. Soc.*, 2002, **124**, 14290–14291; (e) G. Lu, Y. Chen, Y. Zhang, M. Bao, Y. Bian, X. Li and J. Jiang, *J. Am. Chem. Soc.*, 2008, **130**, 11623–11630; (f) Y. Gao, X. Zhang, C. Ma, X. Li and J. Jiang, *J. Am. Chem. Soc.*, 2008, **130**, 17044–17052.